Site-Directed Mutations at Phenylalanine-190 of Manganese Peroxidase: Effects on Stability, Function, and Coordination†

Katsuyuki Kishi,‡ Dean P. Hildebrand,§ Margo Kusters-van Someren,‡,|| Jessica Gettemy,‡ A. Grant Mauk,§ and Michael H. Gold*,‡

Department of Chemistry, Biochemistry, and Molecular Biology, Oregon Graduate Institute of Science and Technology, Portland, Oregon 97291-1000, and Department of Biochemistry and Molecular Biology, University of British Columbia, Vancouver, British Columbia V6T IZ3, Canada

Received October 18, 1996; Revised Manuscript Received February 6, 1997⊗

ABSTRACT: A series of site-directed mutants, F190Y, F190L, F190I, and F190A, in the gene encoding manganese peroxidase isozyme 1 (*mnp1*) from *Phanerochaete chrysosporium* was generated by overlap extension with the polymerase chain reaction. The mutant genes were expressed in *P. chrysosporium* during primary metabolic growth under the control of the glyceraldehyde-3-phosphate dehydrogenase promoter. The manganese peroxidase variants (MnPs) were purified and characterized by kinetic and spectroscopic methods. At pH 4.5, the UV−vis spectra of the ferric and oxidized states of the mutant proteins were very similar to those of the wild-type enzyme. Steady-state kinetic analyses showed that the apparent K_m and k_{cat} values for Mn^{II} and H_2O_2 also were similar to the corresponding values for the wild-type MnP. The apparent K_m and k_{cat} values for ferrocyanide oxidation by MnP were not affected by the F190Y, F190L, or F190I mutations; however, the apparent K_m value for ferrocyanide oxidation by the F190A mutant MnP was ∼1/8 of that for the wild-type enzyme. Likewise, the apparent k_{cat} value for ferrocyanide oxidation by the MnP F190A mutant was ∼4-fold greater than the corresponding k_{cat} for the wild-type MnP. The stabilities of both the native and oxidized states of MnP were significantly affected by several of the mutations at Phe190. Replacement of Phe190 by either Ile or Ala significantly destabilized the resultant proteins to thermal denaturation. Moreover, the rates of spontaneous reduction of the oxidized intermediates, MnP compounds I and II, were dramatically increased for the F190A mutant relative to the rates observed for the wild-type enzyme. The spectroscopic properties of the wild-type and F190 mutant MnPs were examined as a function of pH. At room temperature, increasing pH from 5.0 to 8.5 induced a Fe^{III} high- to low-spin transition for all of the MnP proteins. This transition may involve direct coordination of the distal His residue to the heme iron to produce bishistidinyl coordination as suggested by magnetic circular dichroism spectroscopy. The pH at which this transition occurred was considerably lower for the F190A and F190I variants and suggests that Phe190 plays a critical role in stabilizing the heme environment of MnP.

White-rot basidiomycete fungi are capable of degrading the plant cell wall polymer lignin (Buswell & Odier, 1987; Gold et al., 1989; Kirk & Farrell, 1987) and a variety of aromatic pollutants (Bumpus & Aust, 1987; Hammel, 1989; Joshi & Gold, 1993; Valli & Gold, 1991; Valli et al., 1992). When cultured under ligninolytic conditions, the lignin-degrading fungus *Phanerochaete chrysosporium* secretes two families of extracellular peroxidases, lignin peroxidase (LiP)[1] and manganese peroxidase (MnP), which, along with an H_2O_2-generating system, comprise the major enzymatic constituents of its extracellular lignin-degrading system (Bao et al., 1994; Buswell & Odier, 1987; Gold & Alic, 1993; Hammel et al., 1993; Kirk & Farrell, 1987; Kuwahara et al., 1984; Wariishi et al., 1991). Both LiP and MnP are able to depolymerize lignin *in vitro* (Bao et al., 1994; Hammel et al., 1993; Wariishi et al., 1991). MnP activity has been found in all lignin-degrading fungi that have been examined (Hatakka, 1994; Orth et al., 1993; Perie & Gold, 1991).

MnP has been purified and characterized biochemically and kinetically (Glenn & Gold, 1985; Glenn et al., 1986; Gold & Alic, 1993; Perie et al., 1996; Wariishi et al., 1989, 1992), and the sequences of cDNA and genomic clones encoding several *P. chrysosporium* MnP isozymes have been determined (Godfrey et al., 1990; Gold & Alic, 1993; Mayfield et al., 1994a; Pease et al., 1989; Pribnow et al.,

† Supported by grants from the National Science Foundation (MCB-9506338 to M.H.G.), the U.S. Department of Energy, Office of Basic Energy Sciences (DE-FG03-96ER20235 to M.H.G.), the U.S. Department of Agriculture (C0121A-01 to M.H.G.), and MRC of Canada (MT-7182 to A.G.M.). The EPR spectrometer, EPR cryostat, and spectropolarimeter were purchased with funds provided by the Protein Engineering Network of Centres of Excellence (to A.G.M.).

* To whom correspondence should be addressed at the Department of Chemistry, Biochemistry, and Molecular Biology, Oregon Graduate Institute of Science and Technology, P.O. Box 91000, Portland, OR 97291-1000. Telephone: 503-690-1076. Fax: 503-690-1464. Email: mgold@admin.ogi.edu.

‡ Oregon Graduate Institute of Science and Technology.

§ University of British Columbia.

|| Present address: Section of Molecular Genetics of Industrial Microorganisms, Wageningen Agricultural University, Dreijenlaan 2, 6703 HA Wageningen, The Netherlands.

⊗ Abstract published in *Advance ACS Abstracts,* April 1, 1997.

[1] Abbreviations: CIP, *Coprinus cinereus* peroxidase; CCP, cytochrome *c* peroxidase; EPR, electron paramagnetic resonance; HRP, horseradish peroxidase; LiP, lignin peroxidase; MCD, magnetic circular dichroism; MnP, manganese peroxidase; MnP1, manganese peroxidase isozyme 1; *mnp*1, gene encoding MnP1; PAGE, polyacrylamide gel electrophoresis; PCR, polymerase chain reaction; rMnP1, recombinant MnP1; SDS, sodium dodecyl sulfate.

S0006-2960(96)02627-X CCC: $14.00

1989). Spectroscopic studies and DNA sequences suggest that the heme environment of MnP is similar to that of other plant and fungal peroxidases (Banci et al., 1992; Dunford & Stillman, 1976; Glenn et al., 1986; Harris et al., 1991; Mino et al., 1988; Pribnow et al., 1989; Wariishi et al., 1988). Kinetic and spectroscopic characterization of the oxidized intermediates, MnP compounds I and II, indicates that the catalytic cycle of MnP is similar to that of HRP and LiP (Glenn et al., 1986; Gold et al., 1989; Renganathan & Gold, 1986; Wariishi et al., 1988, 1989, 1992). However, MnP is unique in its ability to oxidize Mn^{II} to Mn^{III} (Glenn & Gold, 1985; Glenn et al., 1986; Wariishi et al., 1992). The enzyme-generated Mn^{III} is stablized by organic acid chelators such as oxalate which is secreted by the fungus (Kishi et al., 1994; Kuan et al., 1993; Wariishi et al., 1992). The Mn^{III}−oxalate complex, in turn, oxidizes substrates such as lignin substructure model compounds (Tuor et al., 1992), synthetic lignin (Bao et al., 1994; Wariishi et al., 1991), and aromatic pollutants (Joshi & Gold, 1993; Valli & Gold, 1991; Valli et al., 1992).

It has been proposed that a unique Mn binding site observed in the MnP crystal structure (Sundaramoorthy et al., 1994) is involved in the oxidation of Mn^{II}. The Mn binding ligands in this proposed binding site are Glu35, Glu39, Asp179, a heme propionate, and two H_2O molecules (Sundaramoorthy et al., 1994). Using an homologous expression system (Mayfield et al., 1994b) for producing recombinant MnP, we carried out site-directed mutagenesis on the proposed Mn^{II} binding site ligands (Kishi et al., 1996; Kusters-van Someren et al., 1995). The results confirmed that Glu35, Glu39, and Asp179 are Mn^{II} ligands and that the proposed Mn^{II} binding site is the productive site (Kishi et al., 1996; Kusters-van Someren et al., 1995).

Other than this unique Mn binding site, the heme environment of MnP appears to be similar to those of other plant and fungal peroxidases (Edwards et al., 1993; Sundaramoorthy et al., 1994). All of the catalytic residues, including the distal His and Arg and the proximal His and Asp, are conserved in MnP, LiP, HRP, CCP, and CIP (Edwards et al., 1993; Finzel et al., 1984; Gold & Alic, 1993; Kunishima et al., 1994; Petersen et al., 1994; Piontek et al., 1993; Poulos et al., 1993; Sundaramoorthy et al., 1994). In addition, as in both HRP and LiP (Edwards et al., 1993; Piontek et al., 1993; Poulos et al., 1993), MnP has two Phe residues (Phe45 and Phe190) in the heme pocket, whereas both CCP and ascorbate peroxidase contain Trp residues at these positions (Finzel et al., 1984; Patterson & Poulos, 1995). CIP has a Leu (Kunishima et al., 1994; Petersen et al., 1994) replacing the proximal Phe (Phe190 in MnP1). In addition, comparison of the LiP and MnP crystal structures (Edwards et al., 1993; Piontek et al., 1993; Poulos et al., 1993; Sundaramoorthy et al., 1994) indicates that the orientations of the plane of the proximal Phe residue of the two enzymes are different. Although the role of the proximal Phe190 in MnP has not been elucidated, it could play a role in protein folding or stability, heme insertion, or stability of the enzyme-oxidized intermediates. In this report, we have replaced the proximal Phe190 with Tyr, Leu, Ile, and Ala to examine the role of this amino acid residue in the MnP reaction.

MATERIALS AND METHODS

Organisms. *P. chrysosporium* wild-type strain OGC101, auxotrophic strain OGC107-1 (Ade1), and prototrophic transformants were maintained as described previously (Alic et al., 1990). *Escherichia coli* XL1-Blue and DH5αF′ were used for subcloning plasmids.

Oligodeoxyribonucleotides. Each of four oligonucleotides were used for site-directed mutagenesis of Phe190 of the *mnp1* gene (Godfrey et al., 1990; Pribnow et al., 1989). Oligonucleotides $B1_{norm}$ and $D1_{rev}$ were 17-mers, prepared as described previously (Kusters-van Someren et al., 1995). Oligonucleotides $Y190_{norm}$, $L190_{norm}$, and $I190_{norm}$ were 28-mers, and $A190_{norm}$, $A190_{rev}$, $Y190_{rev}$, $L190_{rev}$, and $I190_{rev}$ were 27-mers. $Y190_{norm}$, $L190_{norm}$, and $I190_{norm}$ spanned nucleotides 874−901, and $A190_{norm}$ spanned nucleotides 874−900. $A190_{rev}$, $Y190_{rev}$, $L190_{rev}$, and $I190_{rev}$ spanned nucleotides 890−864. Oligonucleotides were synthesized at the Center for Gene Research and Biotechnology, Oregon State University, Corvallis, OR. Oligonucleotides 190_{norm} and 190_{rev} contained the preferred codon and anticodon (Ritch & Gold, 1992), respectively, for corresponding amino acid residues: GCC for A190, TAC for Y190, CTC for L190, and ATC for I190, replacing TTT encoding Phe190.

Site-Directed Mutagenesis by PCR. 554 bp *Bpu*1102I−*Dra*III fragments containing the F190A, F190Y, F190L, and F190I mutations were generated by overlap extension (Ho et al., 1989; Kusters-van Someren et al., 1995) using the polymerase chain reaction (PCR). Two partially overlapping fragments were generated using either oligonucleotides $B1_{norm}$ and $A190_{rev}$ (or $Y190_{rev}$, $L190_{rev}$, or $I190_{rev}$) or oligonucleotides $A190_{norm}$ (or $Y190_{norm}$, $L190_{norm}$, or $I190_{norm}$) and $D1_{rev}$ under the conditions described (Kusters-van Someren et al., 1995). These fragments were combined and used as template DNA in a second reaction with oligonucleotides $B1_{norm}$ and $D1_{rev}$ to generate a 608 bp PCR fragment as described (Kusters-van Someren et al., 1995). The final PCR product was analyzed by agarose gel electrophoresis, excised, purified as described (Kusters-van Someren et al., 1995), and digested with *Bpu*1102I and *Dra*III (New England Biolabs).

Construction of pAGM3, -5, -10, and -13. The *Bpu*1102I−*Dra*III fragments containing the F190 mutations were subcloned into pGM1 (Kusters-van Someren et al., 1995; Mayfield et al., 1994b), containing unique *Bpu*1102I and *Dra*III sites, replacing the wild-type *mnp1* fragment with the mutant fragment, to generate pGM3 (F190Y), pGM5 (F190I), pGM10 (F190L), and pGM13 (F190A). The entire *Bpu*1102I−*Dra*III fragments were analyzed by double-stranded DNA sequencing as described (Kusters-van Someren et al., 1995). Subsequently, the 4.0-kb *Xba*I−*Eco*RI fragments of pGM3, -5, -10, and -13, containing the *gpd* promoter and the mutated *mnp1* gene, were subcloned into pOGI18 (Godfrey et al., 1994), generating pAGM3, -5, -10, and -13, respectively. The presence of the mutations in pAGM3, -5, -10, and -13 was confirmed by double-stranded DNA sequencing, using oligonucleotide $B1_{norm}$ as a primer.

Transformation of Phanerochaete chrysosporium. *P. chrysosporium* strain Ade1 (Gold et al., 1982) was transformed as described previously (Alic et al., 1990), using 1 μg of pAGM3, -5, -10, or -13 as transforming DNA. Transformants were transferred to minimal slants (Alic et al., 1990) to confirm adenine prototrophy and, subsequently, were assayed for MnP activity with an *o*-anisidine plate assay as described (Mayfield et al., 1994b). Transformants showing the greatest activity as detected by the plate assay were purified by fruiting as described (Alic et al., 1987).

Production and Purification of the MnP Mutant Proteins. The MnP mutant proteins were produced under primary metabolic conditions when endogenous *mnp* genes were not expressed, as described previously (Kusters-van Someren et al., 1995; Mayfield et al., 1994b), except that cultures were grown at 28 °C on a rotary shaker (150 rpm) for 3 days. The mutant proteins were purified by a combination of phenyl-sepharose CL-6B column chromatography, Cibacron Blue 3GA agarose column chromatography, and FPLC with a Mono Q column (Pharmacia), as described previously (Kishi et al., 1996; Mayfield et al., 1994b).

SDS−PAGE and Western Analysis. Sodium dodecyl sulfate−polyacrylamide gel electrophoresis (SDS−PAGE) was performed with a 12% Tris−glycine gel system (Laemmli, 1970) and a Mini-Protean II apparatus (Bio-Rad). The gels were stained with Coomassie blue. For Western (immunoblot) analysis, proteins were electroblotted onto nitrocellulose (Micron Separations, Inc.), and MnP proteins were detected as described (Pribnow et al., 1989).

Enzyme Assays and Spectroscopic Procedures. Mn^{II} oxidation by MnP was measured by following the formation of Mn^{III}−malonate as described (Wariishi et al., 1992). The oxidation of ferrocyanide by MnP was followed at 420 nm using the extinction coefficient for ferricyanide of 1.02 mM^{-1} cm^{-1} (Schellenberg & Hellerman, 1958). UV−vis absorption spectra of the various oxidation states of MnP mutant proteins were recorded at 10 °C with a Shimadzu UV-260 spectrophotometer fitted with a circulating water bath. The enzyme was maintained in 20 mM potassium malonate, pH 4.5. The ionic strength of the buffers was adjusted to 0.1 M with K_2SO_4. Enzyme concentrations were determined at 406 nm with an extinction coefficient of 129 mM^{-1} cm^{-1} (Glenn & Gold, 1985). MnP compounds I and II were prepared as described (Kusters-van Someren et al., 1995).

Spectrophotometric pH titrations were carried out by addition of small volumes of 2 M NaOH solution to protein solutions (10 μM) prepared in sodium phosphate buffer (0.1 M, 20 °C). The resulting titration data were fitted by the nonlinear least-squares program Scientist (MicroMath, Orem, UT) to determine the pK_as indicated by the pH-dependent changes in absorbance.

Steady-State Kinetics and Stability Measurements. The apparent K_m and k_{cat} values of the variant enzymes for Mn^{II} and ferrocyanide were determined as described (Kusters-van Someren et al., 1995; Mayfield et al., 1994b). Reaction mixtures contained MnP protein (0.5 μg/mL), H_2O_2 (0.1 mM), and $MnSO_4$ (0.02−0.5 mM) or ferrocyanide (0.1−1.0 mM for F190A and 1.0−5.0 mM for others) in 50 mM sodium malonate, pH 4.5. Apparent K_m values of the mutant enzymes for H_2O_2 were determined as described (Kusters-van Someren et al., 1995; Mayfield et al., 1994b).

The thermal denaturation of MnP proteins was measured by following the absorbance decrease at the Soret maximum at 406 nm. Reaction mixtures contained 2 μM MnP in 20 mM potassium malonate, pH 4.5. The ionic strength of the solutions was adjusted to 0.1 M with K_2SO_4.

Magnetic Circular Dichroism (MCD) Spectroscopy. MCD spectra were acquired with a Jasco Model J-720 spectropolarimeter and a 1.5 T electromagnet (Alpha Magnetics). The samples were placed in a 3-mL quartz cuvette (1-cm path length), and the cuvette was placed into a water-jacketed cell holder maintained at 298 K. Each spectrum represents an average of six scans (300−700 nm). Protein samples ([wild-type MnP] = 8.7 μM and [F190I] = 7.4 μM) for MCD spectroscopy were prepared in 100 mM sodium phosphate buffer, pH 4.5. The pH of the samples was adjusted by addition of small volumes of 1 M sodium hydroxide solution directly to the cuvette.

Electron Paramagnetic Resonance (EPR) Spectroscopy. EPR spectra of wild-type MnP were obtained at X-band frequencies with a Bruker Model ESP 300E spectrometer equipped with an Oxford Instruments Model 900 liquid helium cryostat, an Oxford Instruments Model ITC4 temperature controller, and a Hewlett-Packard Model 5352B frequency counter. The experimental conditions used were 4 K, microwave power 0.5 mW, microwave frequency 9.45 GHz, modulation frequency 100 kHz, and modulation amplitude 0.5 mT. Enzyme samples for EPR spectroscopy were exchanged into 100 mM sodium phosphate buffer of the appropriate pH through repeated dilution and concentration by centrifugal ultrafiltration with an Amicon microconcentrator (Centricon-10). The final concentration of the protein samples was 1.3 mM.

Chemicals. Phenyl-Sepharose CL-6B, Cibacron Blue 3GA agarose, potassium ferrocyanide, and H_2O_2 (30% solution) were obtained from Sigma. All other chemicals were reagent grade. Solutions were prepared using deionized water obtained from a Milli Q purification system (Millipore).

RESULTS

Expression and Purification of Mutant Proteins. The F190Y, F190I, F190L, and F190A mutations were confirmed by double-stranded DNA sequencing of the altered restriction fragments in pGM3, -5, -10, and -13 and in the complete transformation vectors, pAGM3, -5, -10, and -13, respectively. Prototrophic transformants with detectable MnP activity in the plate assay were purified by fruiting as described (Alic et al., 1987). When incubated at 28 °C, the purified transformants expressed extracellular mutant MnP protein within 3 days of growth in liquid, HCHN shake cultures, conditions under which endogenous MnP was not expressed. The amount of variant protein secreted by the F190Y, F190L, and F190I transformants, as assayed by monitoring the formation of the Mn^{III}−malonate complex (Wariishi et al., 1992), was approximately the same as that of recombinant wild-type MnP1 (rMnP1) (Mayfield et al., 1994b). However, the F190A transformants had 10% of the rMnP1 level of activity. Furthermore, the F190Y, F190L, and wild-type transformant exhibited essentially the same amount of MnP activity when grown either at 28 or at 37 °C, whereas the F190I and F190A transformants produced only trace amounts of MnP activity when grown at 37 °C, suggesting that the MnP F190I and F190A proteins were unstable at this temperature. The MnP mutant proteins were purified using phenyl-sepharose, Blue Agarose, and Mono Q chromatographies (Kishi et al., 1996; Kusters-van Someren et al., 1995; Mayfield et al., 1994b). In each case, the major variant protein peak eluted from the Mono Q column at essentially the same position as rMnP1 (Mayfield et al., 1994b). Furthermore, the molecular masses (46 kDa), as determined by SDS−PAGE, of the MnP variant proteins were identical to those of rMnP1 (data not shown) (Mayfield et al., 1994b).

Spectral Properties of MnP Mutant Proteins. For each of the variant proteins, the Soret band at 406 nm rapidly

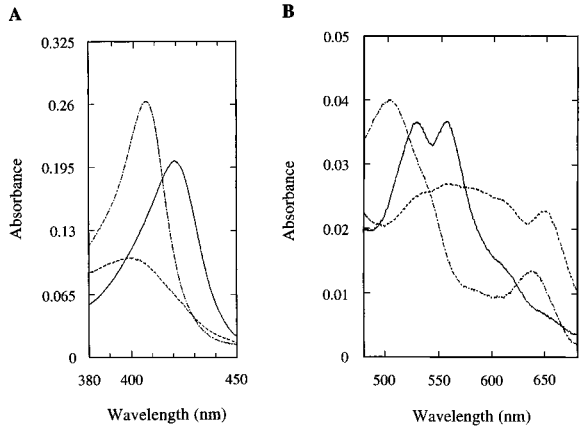

FIGURE 1: Electronic absorption spectra of oxidized states of MnP F190Y: native enzyme (− · −), compound I (- - -), and compound II (—). Spectra were recorded in 20 mM potassium malonate, pH 4.5 (μ = 0.1), at 10 °C. The enzyme concentrations were 2 μM (A, Soret spectra) and 4 μM (B, visible spectra). MnP F190Y compound I was prepared by adding 1 equiv of H_2O_2 to native MnP F190Y. MnP F190Y compound II was prepared by the successive additions of 1.0 equiv of H_2O_2 and 1.0 equiv of potassium ferrocyanide to the native enzyme.

Table 1: Absorbance Maxima (nm) of Native and Oxidized Intermediates of Wild-Type MnP1 and MnP F190 Mutants[a]

enzyme	native	compound I	compound II
wild-type MnP	406, 502, 636	398, 558, 617 (sh),[b] 650	420, 528, 555
MnP F190Y	406, 502, 636	398, 557, 617 (sh),[b] 650	420, 528, 555
MnP F190L	405, 502, 636	397, 558, 617 (sh),[b] 650	420, 528, 555
MnP F190I	405, 501, 635	397, 557, 615 (sh),[b] 468	418, 528, 555
MnP F190A	405, 501, 638	397, 557, 615 (sh),[b] 648	418, 527, 555

[a] Electronic absorption spectra were recorded in 20 mM potassium malonate, pH 4.5 (μ = 0.1), at 10 °C. [b] Shoulder.

decreased and blue-shifted to yield a band at 397 nm following the addition of 1.0 equiv of H_2O_2 to the native enzyme. In the visible region, compound I displayed a peak at 650 nm with a broad absorption at 530−600 nm (Figure 1). Upon the addition of 1.0 equiv of ferrocyanide to the mutant MnP compounds I, compound II spectra, with maxima at 420, 528, and 555 nm, appeared (Figure 1). The electronic absorption maxima of compounds I and II for each of the MnP variant proteins were essentially identical to those of the wild-type enzyme (Table 1).

Steady-State Kinetics. Under steady-state conditions, linear Lineweaver−Burk plots were obtained over a range of Mn^{II}, ferrocyanide, and H_2O_2 concentrations in 50 mM malonate, pH 4.5 (data not shown). The apparent K_m values for H_2O_2 (∼40 μM) and Mn^{II} (∼80 μM) for the MnP variant proteins were similar to those for wild-type MnP1 (Table 2). The apparent k_{cat} values of the variant proteins for Mn^{II} [(2.4−2.9) × 10^2 s^{-1}] also were similar to those for wild-type MnP1. In addition, the apparent K_m (∼3.5 mM) and k_{cat} (∼4.0 s^{-1}) values for ferrocyanide for the F190Y, F190L, and F190I variant proteins were similar to those for the wild-type MnP1 (Table 2). In contrast, the MnP F190A apparent K_m value of 0.42 mM for ferrocyanide was about one-eighth of that for wild-type MnP1, and the MnP F190A apparent k_{cat} value (14.6 s^{-1}) for ferrocyanide was ∼4 times higher than for the wild-type MnP1 (Table 2).

Thermal Denaturation of MnP F190 Mutant Proteins. The thermal denaturation of the MnP variants was followed over a range of temperatures in 20 mM potassium malonate, pH 4.5. Figure 2 shows the natural log plot of the change in absorbance at 406 nm versus time at 49 °C for wild-type MnP and for the F190Y, F190L, and F190I proteins, according to the first-order expression:

$$\ln |A_t - A_\infty| = -kt + \ln |A_0 - A_\infty| \qquad (1)$$

where A_0, A_t, and A_∞ are the Soret absorbance at times 0, t, and the end point, respectively. The rate constants for denaturation (k_{den}) of the MnP proteins were determined from the slopes of the plots, and half-lives ($T_{1/2}$) were calculated for each variant. The $T_{1/2}$ value for the MnP F190I variant at 49 °C (∼30 s) was ∼0.1 that observed for the wild-type MnP and for the MnP F190Y and F190L variant proteins (∼330 s). The MnP F190A variant was denatured completely within 5 s at 49 °C (data not shown).

Table 2: Steady-State Kinetic Parameters of Wild-Type MnP1, MnP F190Y, MnP F190L, MnP F190I, and MnP F190A[a]

	K_m (μM)			k_{cat} (s^{-1})	
	Mn^{II}	H_2O_2	$Fe(CN)_6$	Mn^{II}	$Fe(CN)_6$
wild-type MnP	83	39	3.5×10^3	2.9×10^2	4.0
MnP F190Y	80	41	3.8×10^3	2.8×10^2	4.2
MnP F190L	75	41	3.5×10^3	2.9×10^2	3.9
MnP F190I	78	39	3.4×10^3	2.6×10^2	3.4
MnP F190A	74	39	4.2×10^2	2.4×10^2	14.6

[a] Reactions were carried out in 50 mM sodium malonate, pH 4.5, at room temperature. The apparent K_m and k_{cat} for Mn^{II} and ferrocyanide were determined in the presence of 0.1 mM H_2O_2. The apparent K_m for H_2O_2 was determined in the presence of 0.5 mM Mn^{II}.

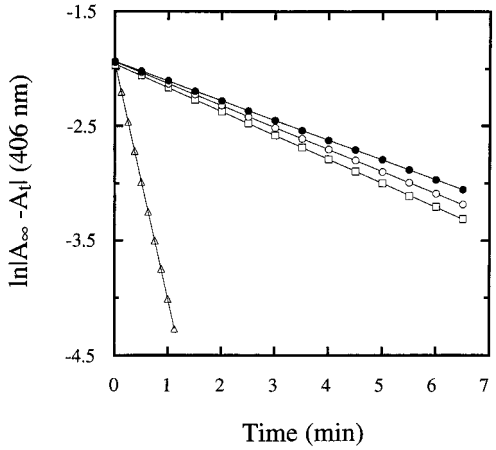

FIGURE 2: First-order plots for the thermal denaturation of wild-type MnP (●), MnP F190Y (○), F190L (□), and F190I (△) at 49 °C in 20 mM potassium malonate, pH 4.5 (μ = 0.1). The thermal denaturation of MnP proteins was followed at 406 nm.

Arrhenius plots for denaturation (ln k_{den} versus 1/T) were linear for all forms of MnP studied (Figure 3). The activation energies, E_a, derived from the slopes of these plots were very similar (∼80 kcal/mol) for the wild-type and MnP F190 variants. However, the temperature dependence in the MnP F190I and F190A variants of the rate of denaturation is shifted significantly with respect to those of the wild-type, F190Y, and F190L MnPs.

Stability of MnP Compounds I and II. MnP compound I spontaneously reduced to compound II at pH 4.5 as observed from the increase in absorbance at 417 nm, an isosbestic point in the spectra of compound II and the native protein. The plots of the natural log of absorbance versus time

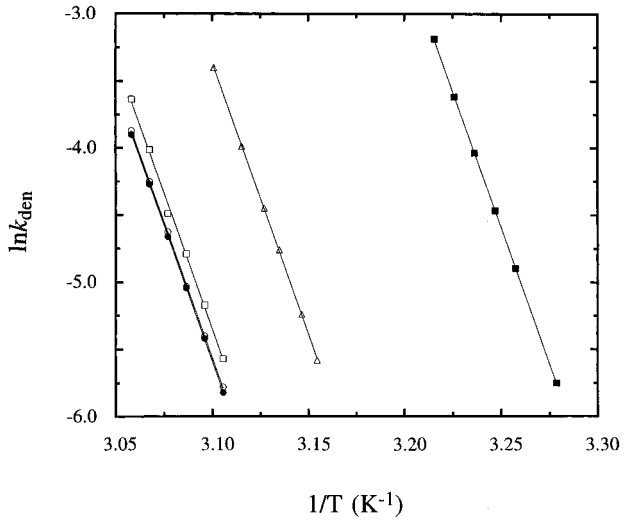

FIGURE 3: Arrhenius plot for the thermal denaturation of wild-type MnP (●), MnP F190Y (○), F190L (□), F190I (△), and F190A (■).

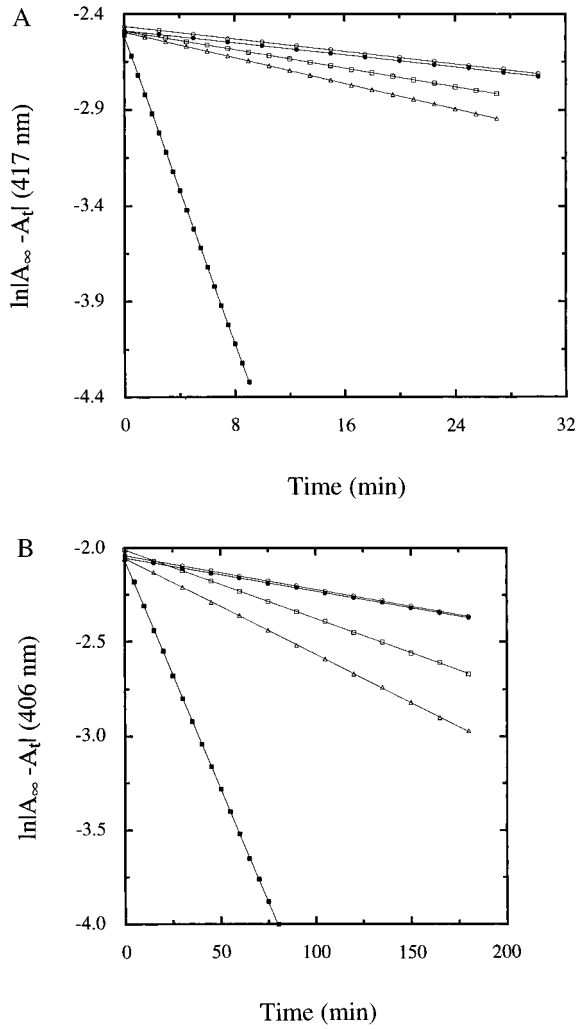

FIGURE 4: First-order plot for the spontaneous reductions of compound I (A) and compound II (B) of wild-type MnP (●), MnP F190Y (○), F190L (□), F190I (△), and F190A (■). The spontaneous reductions of compounds I and II were followed at 417 and 406 nm, respectively. MnP compounds I and II were prepared at 10 °C as described in the legend to Figure 1.

(eq 1) exhibited a linear relationship (Figure 4A) from which the rate constants for spontaneous reduction of compounds I to II were calculated.

Table 3: Spontaneous Reduction of Compounds I and II of the MnP Variants[a]

	compound I to II[b]		compound II to native[c]	
	k_1 (s^{-1})	$T_{1/2}$ (min)	k_2 (s^{-1})	$T_{1/2}$ (min)
wild-type MnP1	1.3×10^{-4}	89	3.0×10^{-5}	3.9×10^{2}
MnP F190Y	1.3×10^{-4}	89	3.0×10^{-5}	3.9×10^{2}
MnP F190L	2.4×10^{-4}	48	6.2×10^{-5}	1.9×10^{2}
MnP F190I	2.8×10^{-4}	41	7.6×10^{-5}	1.5×10^{2}
MnP F190A	3.4×10^{-3}	3.4	4.1×10^{-4}	0.28×10^{2}

[a] Reactions were carried out in 20 mM potassium malonate, pH 4.5, at 10 °C (ionic strength adjusted to 0.1 M with K_2SO_4). [b] The conversion of compound I to II was followed at 417 nm. [c] The conversion of compound II to native protein was followed at 406 nm.

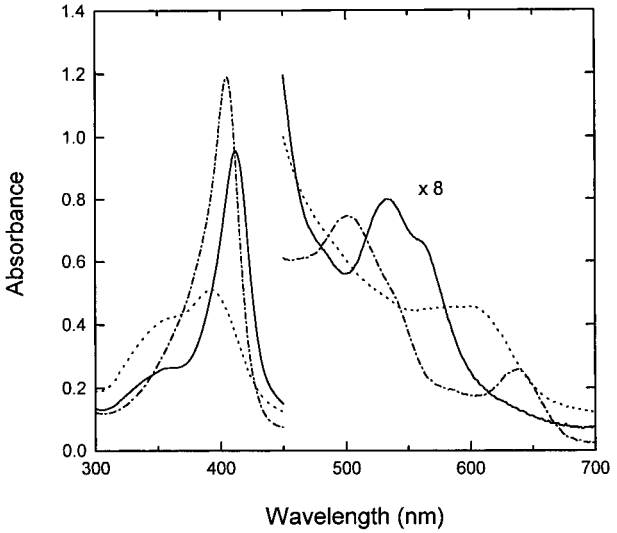

FIGURE 5: Electronic absorption spectra of MnP F190I in 100 mM sodium phosphate buffer (20 °C) at selected pHs: pH 5.3 (—•—); pH 8.2 (—); pH 10.2 (- - -).

The spontaneous reduction of compound II also was measured for the MnP variants by following the increase in absorbance of the Soret maximum at 406 nm (Figure 4B). The rate constants for spontaneous reduction of compounds I and II of the F190I and F190L variants were ~2-fold greater than those determined for the wild-type and F190Y variants (Table 3). Moreover, the rate constants for spontaneous reduction of the F190A compounds I and II were approximately 30- and 13-fold greater, respectively, than those observed for the wild-type MnP compounds I and II (Table 3).

pH-Dependent Shifts in the Electronic Absorption Spectra of MnP F190 Variants. The electronic spectra of the MnP F190I variant exhibited two apparent pH-dependent transitions between pH 5 and 10 (Figure 5). At pH 5.3, the spectrum of the MnP F190I variant was typical of a high-spin heme Fe^{III} species (λ_{max} = 405, 501, 635 nm). At pH 8.2, the electronic spectrum was characteristic of a hexacoordinate low-spin Fe^{III} species with maxima at 412, 534, and 560 nm that suggested the presence of a bishistidinyl coordination environment for the heme iron (Ferrer et al., 1994; Turano et al., 1995; Vitello et al., 1992). Above pH 8.2, further spectroscopic changes were observed, probably owing to the alkaline denaturation of the MnP protein. Similar transitions were observed in the electronic spectra of the wild-type MnP and MnP F190Y, F190L, and F190A variants (data not shown). The pH-dependent changes in absorbance were monitored at 560 nm (Figure 6) where the

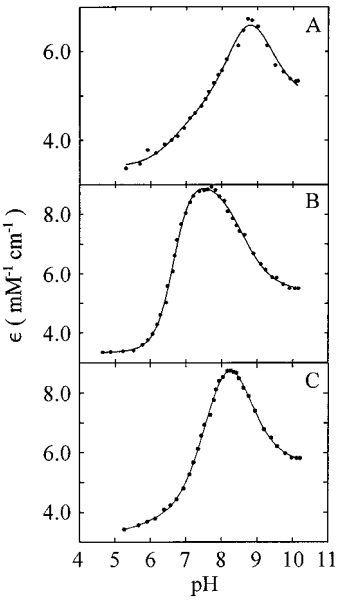

FIGURE 6: Dependence of the absorbance at 560 nm on pH for (A) wild-type MnP, (B) F190A, and (C) F190I in 100 mM sodium phosphate buffer (20 °C). The solid lines represent the nonlinear fits of these data to three single proton processes for wild-type MnP F190I and F190A. Apparent pK_a values for wild-type and variant forms of MnP are listed in Table 4.

Table 4: Apparent pK_a Values of the pH-Dependent Transitions of Wild-Type MnP, MnP F190Y, F190L, F190I, and F190A in 100 mM Sodium Phosphate Buffer (20 °C)

enzyme	pK_{a1}	pK_{a2}	pK_{a3}
wild-type MnP	6.67 ± 0.18	8.39 ± 0.10	9.15 ± 0.13
MnP F190Y	6.78 ± 0.14	8.62 ± 0.07	8.91 ± 0.14
MnP F190L	6.58 ± 0.26	8.67 ± 0.07	8.89 ± 0.06
MnP F190I	5.69 ± 0.65	7.71 ± 0.04	8.60 ± 0.04
MnP F190A	6.21 ± 0.12	7.08 ± 0.16	8.55 ± 0.05

changes in absorbance were most pronounced (Figure 5). The pH-linked transitions of all the MnP variants could be fitted to three proton processes. The pK_a values derived from these analyses are listed in Table 4. Whereas the pK_a values for wild-type MnP, MnP F190Y, and MnP F190L were similar to each other, the pK_a values obtained for MnPs F190I and F190A, particularly the pK_{a1} and pK_{a2} values, were significantly lower (Table 4).

MCD Spectroscopy. To assess the basis for the changes observed in the electronic spectrum of MnP with pH, MCD spectra were obtained at ambient temperature for both the wild-type and variant (F190I) enzymes (Figure 7). The MCD spectrum of wild-type MnP exhibited significant pH-dependent changes (Figure 7A). The spectrum of the native enzyme (pH 5.9) exhibited a derivative-shaped Soret band (peak, 399 nm; crossover, 408 nm; trough, 418 nm). The visible region (450−700 nm) exhibited additional maxima at ∼482 and 650 nm, as well as an additional derivative-shaped band (peak, 529 nm; crossover, 538 nm; trough, 551 nm). The MCD features in the visible region resembled those observed for other high-spin heme proteins with a proximal histidine residue [e.g., HRP (Nozawa et al., 1976) and myoglobin (Vickery et al., 1976a)]. At pH 7.8, wild-type MnP exhibited little change in the position of the Soret band (peak, 402 nm; crossover, 411 nm; trough, 421 nm), but a significant increase in intensity of this band that is consistent with an increase in the low-spin component of the heme iron (Vickery et al., 1976a). At this pH, a new

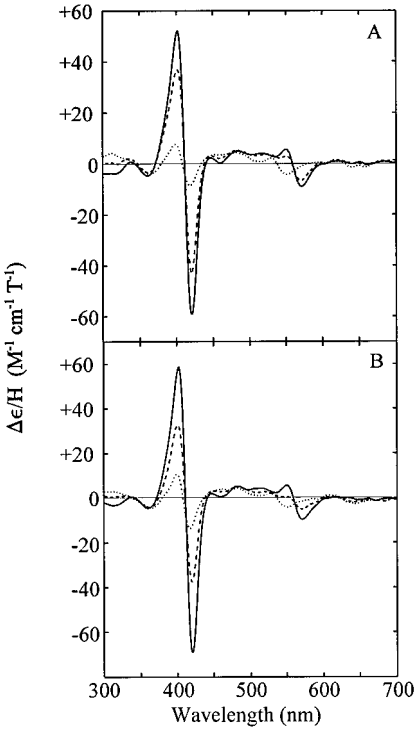

FIGURE 7: Visible MCD spectra (298 K) of ferric manganese peroxidase in 100 mM sodium phosphate buffer. (A) Wild-type enzyme at pH 5.9 (···), pH 6.9 (- - -), and pH 7.8 (—). (B) The F190I variant at pH 5.9 (···), pH 6.5 (- - -), and pH 7.5 (—).

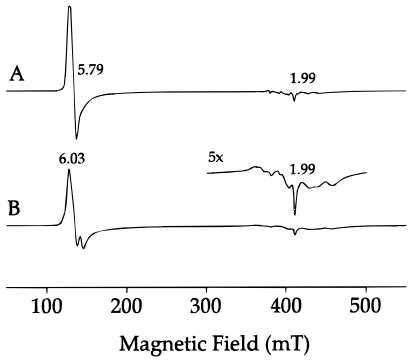

FIGURE 8: X-band EPR spectra (4 K) of wild-type manganese peroxidase (100 mM sodium phosphate buffer) at (A) pH 4.5 and (B) pH 8.0. The expanded region shows the spectrum of the minor, low-spin component.

derivative-shaped feature appeared (peak, 550 nm; crossover, 559 nm; trough, 571 nm) that resembled similar features observed in the MCD spectra of heme proteins with bisimidazole axial coordination, such as cytochrome b_5 and the imidazole complexes of myoglobin and cytochrome *c* (Vickery et al., 1976b). The pH-dependent changes observed in the spectrum of the F190I MnP variant (Figure 7B) were essentially identical to those of the wild-type enzyme and confirm that the conformational change observed for this variant was unaltered by the F190I substitution at the active site. These pH-dependent changes in the MCD spectra were similar to those reported previously for a variant of CCP (Turano et al., 1995).

EPR Spectroscopy. The EPR spectra (4 K) of wild-type MnP at pH 4.7 and 8.0 are shown in Figure 8. At low pH, the native Mn-depleted enzyme exhibits a single high-spin axially symmetric species with *g* values of 5.79 and 1.99 as reported previously (Mino et al., 1988). These properties

differentiate MnP and LiP from other well-studied peroxidases (e.g., CCP) that have more rhombically distorted electronic environments (Yonetani & Anni, 1987). Unexpectedly, at 4 K, wild-type MnP remained almost completely high-spin at high pH ($g \sim 6.03$ and 1.99) and exhibited only a trace of low-spin component(s), the identity of which is uncertain (Figure 8B, expanded region). In contrast, the MCD spectrum acquired at ambient temperature was that of a predominantly low-spin species at pH 7.8. Therefore, wild-type MnP exhibited complex temperature-dependent changes in axial ligation, in which the distal histidine was displaced at low temperatures. The lack of correlation between the EPR spectrum of the enzyme at cryogenic temperature and the electronic and MCD spectra obtained at ambient temperature has been noted previously for variants of cytochrome *c* peroxidase (Ferrer et al., 1994; Turano et al., 1995; Bujons et al., 1997) and for a variant of myoglobin (Lloyd et al., 1995). Comparison of spectra obtained for alkaline and acidic solutions of MnP of comparable concentration (~1.3 mM) indicates that the intensity of the high-spin signal of the alkaline form of the enzyme (pH 8) is only ~60% of the intensity of the low-pH form (pH 4.5). This difference is apparent in Figure 8. The remaining spin in the spectrum of the alkaline enzyme is presumably accounted for in the mixture of low-spin species observed at high pH.

DISCUSSION

Although the catalytic cycle of MnP is similar to that of other plant and fungal peroxidases (Dunford & Stillman, 1976; Gold et al., 1989; Renganathan & Gold, 1986; Wariishi et al., 1988, 1989), this enzyme is unique in that it oxidizes Mn^{II} to Mn^{III} (Glenn et al., 1986; Wariishi et al., 1989, 1992). Mn^{III}, complexed with an organic acid such as oxalate, diffuses from the enzyme to oxidize the terminal organic substrate (Glenn et al., 1986; Tuor et al., 1992). Whereas phenolic compounds can be oxidized directly by MnP compound I, direct oxidation of phenols by MnP compound II is 3 orders of magnitude slower than the oxidation of Mn^{II} by compound II (Kishi et al., 1996; Kusters-van Someren et al., 1995; Wariishi et al., 1988, 1989). Thus, Mn^{II} is required to complete the MnP catalytic cycle (Wariishi et al., 1988, 1989). The three-dimensional structure of MnP suggests that the ability of MnP to oxidize Mn^{II} is due to its unique Mn binding site (Sundaramoorthy et al., 1994) which includes three acidic amino acid ligands, Asp179, Glu35, and Glu39, and one of the heme propionates. The final two ligands of the hexacoordinate Mn^{II} ion are water molecules. Our recent site-directed mutagenesis analysis of the amino acid ligands to Mn demonstrates that this is the productive Mn binding site (Kishi et al., 1996; Kusters-van Someren et al., 1995).

A variety of studies have shown that the heme environment of MnP is similar to that of other plant and fungal peroxidases (Figure 9) (Gold & Alic, 1993; Mino et al., 1988; Sundaramoorthy et al., 1994). Catalytically important amino acid residues found in plant and fungal peroxidases (Edwards et al., 1993; Finzel et al., 1984; Gold & Alic, 1993; Kunishima et al., 1994; Patterson & Poulos, 1995; Petersen et al., 1994; Piontek et al., 1993; Poulos et al., 1993; Sundaramoorthy et al., 1994), including the distal His46, Arg42, Asn80, and Glu74, and the proximal His173 and Asp242, are all conserved in MnP. In addition to these catalytic amino acid residues, MnP contains two Phe residues in the heme pocket (Figure 9). The proximal Phe residue (F190) is conserved

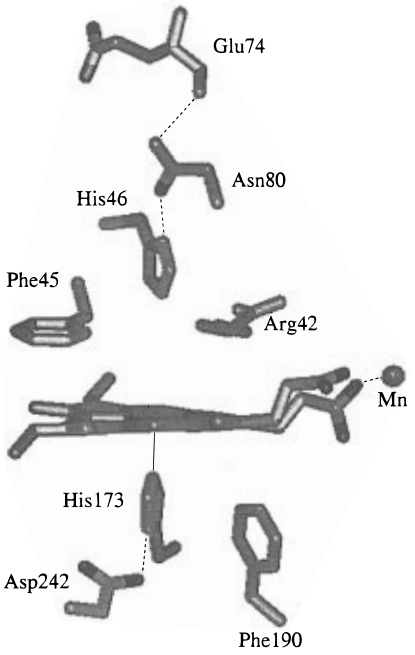

FIGURE 9: Heme environment of MnP (Sundaramoorthy et al., 1994).

in LiP (Edwards et al., 1993; Piontek et al., 1993; Poulos et al., 1993), HRP (Sundaramoorthy et al., 1994), and peanut peroxidase (Schuller et al., 1996). In contrast, both CCP and ascorbate peroxidase have a Trp at this position, and CIP has a Leu (Finzel et al., 1984; Kunishima et al., 1994; Patterson & Poulos, 1995; Petersen et al., 1994). Trp191 in CCP forms an H-bond network through the proximal Asp to the proximal His, which apparently affects the Fe(III)/Fe(II) reduction potential of the heme (Goodin & McRee, 1993; Poulos & Finzel, 1984). In addition, Trp191 in CCP is thought to be the location of the protein-centered radical in compound I (compound ES) (Sivaraja et al., 1989), which is thought to be essential for electron transfer from cytochrome *c* (Mauro et al., 1988). Conversion of Trp191 to a Phe in CCP blocks electron transfer from ferrocytochrome *c* (Mauro et al., 1988). The presence of a less easily oxidizable amino acid residue, such as Phe, at this position, in part explains why compounds I of HRP, LiP, and MnP possess a porphyrin π-cation radical (Dolphin et al., 1971). Although a Trp is located at this position in ascorbate peroxidase (Patterson & Poulos, 1995), a protein-centered Trp radical is not generated in this enzyme. It has been proposed that a cation, possibly a K^+, is located close to the proximal Trp residue in ascorbate peroxidase, preventing Trp oxidation to a cation radical (Patterson & Poulos, 1995; Patterson et al., 1995). To study the role of Phe190 in MnP, we replaced this residue with Trp, Tyr, Leu, Ileu, and Ala.

Our attempts to produce the F190W variant protein have not been successful. This variant is not secreted from the cells as demonstrated by Western immunoblot analysis (data not shown); similarly, MnP activity is not detectable in the extracellular medium or in the intracellular soluble extract of the F190W transformant. The bulky indole ring of the Trp residue may prevent proper folding of this MnP variant. All of the other variant proteins are secreted into the extracellular medium in active form.

The spectrum of wild-type MnP compound I exhibits a Soret band at 397 nm and a peak at 650 nm with a broad

absorption maximum at 530−600 nm (Wariishi et al., 1988). This spectrum is typical of that of an oxyferryl iron with a porphyrin π-cation radical (Dolphin et al., 1971). In contrast, the CCP compound I spectrum is similar to that of HRP compound II (Dunford & Stillman, 1976), a result that presumably reflects the fact that neither derivative possesses a porphyrin π-cation radical. As shown in Figure 1, the electronic spectrum of MnP F190Y compound I is essentially identical to that of wild-type MnP, suggesting that this variant also forms a porphyrin π-cation radical. The results summarized in Table 1 demonstrate that the absorption maxima for compounds I and II of each of the other variants are essentially identical to those of the wild-type enzyme, suggesting that each of the variants undergoes a normal catalytic cycle. The MnP F190Y variant and the wild-type MnP enzyme exhibit identical steady-state kinetic properties (Table 2), and the stabilities of compounds I of the wild type and F190Y variant are identical (Figure 4A and Table 3). All of these results strongly suggest that the MnP F190Y variant forms a normal porphyrin π-cation radical instead of a phenoxy radical at Tyr, during the catalytic cycle. Recently, the formation of a Tyr radical has been reported for the HRP F172Y mutant (Miller et al., 1995). However, in HRP, Phe172 is close to the heme δ-meso edge, whereas Phe190 in MnP may not be in the proper orientation to react with the porphyrin π-cation radical in compound I. In addition, Bonagura et al. (1996) have demonstrated that a stable Trp191 radical cannot be generated in a CCP variant containing a cation binding site near Trp191. Their engineered cation binding site is similar to the proximal Ca^{II} binding site in other peroxidases (Bonagura et al., 1996), suggesting that the proximal Ca^{II} ion, like the K^+ ion in ascorbate peroxidase, prevents the formation of a protein-centered radical in MnP and other peroxidases. This result may explain why a phenoxy radical is not generated at Tyr190 of the F190Y MnP variant.

Since CIP has a Leu in place of Phe190 (Kunishima et al., 1994; Petersen et al., 1994), and CCP and ascorbate peroxidase have a Trp (Finzel et al., 1984; Patterson & Poulos, 1995), peroxidases do not require a proximal Phe residue for catalytic function. Therefore, we mutated MnP Phe190 to Tyr, Leu, Ile, and Ala in an attempt to assess the function of this heme pocket residue. The replacement of Phe190 by Tyr, Leu, Ile, and Ala does not affect significantly the kinetics of the MnP reactions with Mn^{II} and H_2O_2 (Table 2). The apparent K_m values for Mn^{II} and H_2O_2 with all the MnP F190 variants are approximately the same as those for wild-type MnP, suggesting that the mutations at Phe190 do not alter Mn^{II} or H_2O_2 binding. The apparent k_{cat} values for Mn^{II} also are not affected significantly by the mutations, suggesting that Phe190 does not control the rate of electron transfer from Mn^{II}, at least at pH 4.5. In contrast, replacement of Phe190 by Ala significantly changes the apparent K_m and k_{cat} for ferrocyanide (Table 2). The apparent K_m value decreases ~8-fold, and the apparent k_{cat} increases ~4-fold, suggesting that the F190A mutation creates unique access to the heme edge for small molecules such as ferrocyanide. Similarly, replacement of Trp191 with Gly in CCP dramatically increases its binding productivity for imidazole compounds (Fitzgerald et al., 1994).

Both the F190I and F190A variants are significantly less stable than wild-type MnP. The results for the thermal denaturation of the MnP variants (Figures 2 and 3) suggest that MnP F190I and F190A are 1 and 2 orders of magnitude less stable, respectively, than wild-type MnP and the MnP F190Y and F190L variants. The identity of the slopes observed in the Arrhenius plots establishes that the activation energies and enthalpies for denaturation of the wild-type and variant enzymes are identical and that the entropy of activation increases in the order WT ~ F190Y < F190L < F190I ≪ F190A. The entropic origin for destabilization of the I and A variants probably reflects decreased affinity of these variants for heme as recently reported for variants of myoglobin (Hargrove & Olson, 1996). From the three-dimensional structure of the wild-type enzyme (Sundaramoorthy et al., 1994), Phe190 is known to be located on a loop between α-helices F and G. It is possible that changing Phe190 to Ile or Ala alters the conformation of the loop to produce movement of these two α-helices with respect to each other. In addition, a Phe, Tyr or Leu residue at position 190 may have a stabilizing hydrophobic interaction with the heme.

Mutations at Phe190 affect the stability of the MnP intermediates, compounds I and II (Figure 4A,B, Table 3). Although the electronic spectra of compounds I and II of the MnP F190 variants are nearly identical to those of the wild-type MnP (Table 1), higher rates of spontaneous reduction of compounds I and II are observed for several of the variants, particularly MnP F190A. These results suggest that the bulky Phe residue acts as a steric barrier that protects the heme from reducing agents.

The electronic absorption spectra of heme-containing proteins are good indicators of high- and low-spin derivatives of Fe^{III}. The coordination of strong-field ligands such as cyanide generates low-spin derivatives, whereas coordination of weak-field ligands such as fluoride, or penta-coordination, yields high-spin species. Since the energy difference between the high- and low-spin species is small in many heme proteins, mixed-spin Fe^{III} heme species often are observed with the coordination of certain ligands such as water, hydroxide, azide, and imidazole (Palmer, 1985; Smith & Williams, 1968). The Fe^{III} heme of most peroxidases is coordinated to the protein through the imidazole group of a proximal His residue. The spectroscopic differences among the various derivatives of heme proteins result primarily from differences in coordination on the distal side of the Fe^{III}. Fe^{III} heme proteins typically exhibit four bands in the visible region of the electronic spectrum. Two bands, α and β, appear near 570 and 540 nm, respectively, and two ligand-to-metal charge-transfer bands occur near 500 and 630 nm (Palmer, 1985). High-spin derivatives exhibit absorption maxima at the charge-transfer positions, and low-spin derivatives predominantly exhibit α and β bands. Upon increasing the pH, changes in the protein ligands to the heme can be observed. Typically, hexacoordinate aquo-, hydroxy-, and bisimidazole forms are observed for various heme proteins (Iizuka & Yonetani, 1970).

At low pH (pH 4.5), both wild-type MnP and the MnP F190 variants exhibit high-spin species with charge-transfer bands at 500 and 635 nm (Table 1, Figures 1 and 5). Resonance Raman spectroscopic analysis of the wild-type MnP (Kishi et al., 1996; Mino et al., 1988) has demonstrated that MnP is predominantly pentacoordinate with a minor water-ligated hexacoordinate species. With increasing pH, all of the MnP variants are converted to low-spin species with α and β bands near 560 and 532 nm, respectively

(Figure 5). The positions of these α and β bands and the characteristic MCD spectra (Figure 7) (Dawson & Dooley, 1983; Vickery et al., 1976b) suggest that this transition may involve the direct coordination of the distal His to the iron to form a bishistidinyl complex. However, a mixture of hydroxyimidazole and bisimidazole coordination cannot be ruled out at this time. With a further increase of pH, all of the MnP variants undergo denaturation (Figure 5). Although all of the spectra of the MnP variants exhibit similar transitions upon increasing pH (high-spin to low-spin to denaturation), coordination of the distal His46 to the heme iron occurs at a significantly lower pH for the MnP F190I and MnP F190A variants relative to the behavior of wild-type MnP or the MnP F190Y and F190L variants (Figure 6, Table 4). This observation suggests that a presumed hydrogen bond that is responsible for the first transition is weaker in the MnP F190I and F190A variants relative to wild-type MnP and the MnP F190Y and F190L variants. Surprisingly, two pK_a values (pK_{a1} and pK_{a2}), rather than one, are obtained in the high-spin to low-spin transition for all the variants (Table 4), while only two species are observed in this transition by optical absorption and MCD spectroscopies (Figures 5 and 7). The first transition (pK_{a1}) may be due to a conformational change that occurs prior to the coordination of the distal His to the Fe^{III} heme. Although the pH-dependent transition (pK_{a2}) could represent deprotonation of the distal His46, it has been demonstrated that MnP compound I formation with H_2O_2 is independent of pH from pH 3.1 to 8.3 (Wariishi et al., 1989), which suggests that His46 is deprotonated in this pH range and that other amino acid residues may be responsible for the pH-dependent transition of MnP. The protonation status of His181 has been proposed to be linked to the transition between the high-spin and low-spin species of CCP variants (Nozawa et al., 1976; Vitello et al., 1992). In CCP, His181 forms a hydrogen bond with the 7-propionate group of the heme (Edwards & Poulos, 1990; Finzel et al., 1984). A similar H-bond to the heme propionate groups of MnP is not observable in the crystal structure (Sundaramoorthy et al., 1994). In MnP, the heme 7-propionate is hydrogen-bonded to the peptide NH groups of Asp179 and Lys180 and to two water molecules, one of which is coordinated to the Mn^{II}. The 6-propionate apparently interacts with the Mn^{II} ion, the peptide NH group of Arg177, and a water molecule (Sundaramoorthy et al., 1994). The orientation of the 7-propionate in MnP appears to permit formation of an H-bond with the distal Arg42 residue (Sundaramoorthy et al., 1994). These interractions suggest that the high- to low-spin transition of MnP may not be dependent on the interaction of the heme propionate groups with amino acid side chain groups. Although the assignment of the amino acid residues responsible for this high- to low-spin pH transition remains to be clarified, our results suggest that replacement of Phe190 by Ile, or especially Ala, may weaken hydrogen bond(s) involved in protein stability and in the pH-linked spin transition. Furthermore, replacing the bulky Phe residue with certain smaller residues such as Ile or Ala may lead to greater flexibility of the heme in its pocket.

Conclusions. Mutation of the proximal Phe in MnP has little effect on the steady-state kinetic parameters for the substrates H_2O_2 and Mn. However, these mutations result in significant changes in the temperature stability of the variant proteins and in the stability of the oxidized intermediates, compounds I and II. These changes also affect the pH-dependent interconversion of the pentacoordinate, high-spin Fe heme and the hexacoordinate bis-His-ligated low-spin Fe heme species. Furthermore, the F190A variant exhibits an increased ability to oxidize ferrocyanide. Further structural and mechanistic characterizations of these MnP F190 variants are underway.

REFERENCES

Alic, M., Letzring, C., & Gold, M. H. (1987) *Appl. Environ. Microbiol. 53*, 1464−1469.

Alic, M., Clark, E. K., Kornegay, J. R., & Gold, M. H. (1990) *Curr. Genet. 17*, 305−311.

Banci, L., Bertini, I., Pease, E. A., Tien, M., & Turano, P. (1992) *Biochemistry 31*, 10009−10017.

Bao, W., Fukushima, Y., Jensen, K. A., Moen, M. A., & Hammel, K. E. (1994) *FEBS Lett. 354*, 297−300.

Bonagura, C. A., Sundaramoorthy, M., Pappa, H. S., Patterson, W. R., & Poulos, T. L. (1996) *Biochemistry 35*, 6107−6115.

Bujons, J., Dikiy, A., Ferrer, J. C., Banci, L., & Mauk, A. G. (1997) *Eur. J. Biochem. 243*, 72−84.

Bumpus, J. A., & Aust, S. D. (1987) *BioEssays 6*, 166−170.

Buswell, J. A., & Odier, E. (1987) *CRC Crit. Rev. Biotechnol. 6*, 1−60.

Dawson, J. H., & Dooley, D. M. (1983) in *Iron Porphyrins, Part 3* (Lever, A. B. P., & Gray, H. B., Eds.) pp 1−131, VCH Publishers, New York.

Dolphin, D., Forman, A., Borg, D. C., Fajer, J., & Felton, R. H. (1971) *Proc. Natl. Acad. Sci. USA 68*, 614−618.

Dunford, H. B., & Stillman, J. S. (1976) *Coord. Chem. Rev. 19*, 187−251.

Edwards, S. L., & Poulos, T. L. (1990) *J. Biol. Chem. 265*, 2588−2595.

Edwards, S. L., Raag, R., Wariishi, H., Gold, M. H., & Poulos, T. L. (1993) *Proc. Natl. Acad. Sci. USA 90*, 750−754.

Ferrer, J. C., Turano, P., Banci, L., Bertini, I., Morris, I. K., Smith, K. M., Smith, M., & Mauk, A. G. (1994) *Biochemistry 33*, 7819−7829.

Finzel, B. C., Poulos, T. L., & Kraut, J. (1984) *J. Biol. Chem. 259*, 13027−13036.

Fitzgerald, M. M., Churchill, M. J., McRee, D. E., & Goodin, D. B. (1994) *Biochemistry 33*, 3807−3818.

Glenn, J. K., & Gold, M. H. (1985) *Arch. Biochem. Biophys. 242*, 329−341.

Glenn, J. K., Akileswaren, L., & Gold, M. H. (1986) *Arch. Biochem. Biophys. 251*, 688−696.

Godfrey, B. J., Mayfield, M. B., Brown, J. A., & Gold, M. H. (1990) *Gene 93*, 119−124.

Godfrey, B. J., Akileswaren, L., & Gold, M. H. (1994) *Appl. Environ. Microbiol. 60*, 1353−1358

Gold, M. H., & Alic, M. (1993) *Microbiol. Rev. 57*, 605−622.

Gold, M. H., Cheng, T. M., & Mayfield, M. B. (1982) *Appl. Environ. Microbiol. 44*, 996−1000.

Gold, M. H., Wariishi, H., & Valli, K. (1989) *ACS Symp. Ser. 389*, 127−140.

Goodin, D. B., & McRee, D. E. (1993) *Biochemistry 32*, 3313−3324.

Hammel, K. E. (1989) *Enzyme Microb. Technol. 11*, 776−777.

Hammel, K. E., Jensen, K. A., Jr., Mozuch, M. D., Landucci, L. L., Tien, M., & Pease, E. A. (1993) *J. Biol. Chem. 268*, 12274−12281.

Hargrove, M. S., & Olson, J. S. (1996) *Biochemistry 35*, 11310−11318.

Harris, R. Z., Wariishi, H., Gold, M. H., & Ortiz de Montellano, P. R. (1991) *J. Biol. Chem. 266*, 8751−8758.

Hatakka, A. (1994) *FEMS Microbiol. Rev. 13*, 125−135.

Ho, S. N., Hunt, H. D., Horton, R. M., Pullen, J. K., & Pease, L. R. (1989) *Gene 77*, 51−59.

Iizuka, T., & Yonetani, T. (1970) *Adv. Biophys. 1*, 157−182.

Joshi, D., & Gold, M. H. (1993) *Appl. Environ. Microbiol. 59*, 1779−1785.

Kirk, T. K., & Farrell, R. L. (1987) *Annu. Rev. Microbiol. 41*, 465−505.

Kishi, K., Wariishi, H., Marquez, L., Dunford, H. B., & Gold, M. H. (1994) *Biochemistry 33*, 8694−8701.
Kishi, K., Kusters-van Someren, M., Mayfield, M. B., Sun, J., Loehr, T. M., & Gold, M. H. (1996) *Biochemistry 35*, 8986−8994.
Kuan, I.-C., Johnson, K. A., & Tien, M. (1993) *J. Biol. Chem. 268*, 20064−20070.
Kunishima, N., Fukuyama, K., Matsubara, H., Hatanaka, H., Shibano, Y., & Amachi, T. (1994) *J. Mol. Biol. 235*, 331−344.
Kusters-van Someren, M., Kishi, K., Lundell, T., & Gold, M. H. (1995) *Biochemistry 34*, 10620−10627.
Kuwahara, M., Glenn, J. K., Morgan, M. A., & Gold, M. H. (1984)- *FEBS Lett. 169*, 247−250.
Laemmli, U. K. (1970) *Nature 227*, 680−685.
Lloyd, E., Hildebrand, D. P., Tu, K. M., & Mauk, A. G. (1995) *J. Am. Chem. Soc. 117*, 6434−6438.
Mauro, J. M., Fishel, L. A., Hazzard, J. T., Meyer, T. E., Tollin, G., Cusanovich, M. A., & Kraut, J. (1988) *Biochemistry 27*, 6243−6256.
Mayfield, M. B., Godfrey, B. J., & Gold, M. H. (1994a) *Gene 142*, 231−235.
Mayfield, M. B., Kishi, K., Alic, M., & Gold, M. H. (1994b) *Appl. Environ. Microbiol. 60*, 4303−4309.
Miller, V. P., Goodin, D. B., Friedman, A. E., Hartmann, C., & Ortiz de Montellano, P. R. (1995) *J. Biol. Chem. 270*, 18413−18419.
Mino, Y., Wariishi, H., Blackburn, N. J., Loehr, T. M., & Gold, M. H. (1988) *J. Biol. Chem. 263*, 7029−7036.
Nozawa, T., Kobayashi, N., & Hatano, M. (1976) *Biochim. Biophys. Acta 427*, 652−662.
Orth, A. B., Royce, D. J., & Tien, M. (1993) *Appl. Environ. Microbiol. 59*, 4017−4023.
Palmer, G. (1985) *Biochem. Soc. Trans. 13*, 548−560.
Patterson, W. R., & Poulos, T. L. (1995) *Biochemistry 34*, 4331−4341.
Patterson, W. R., Poulos, T. L., & Goodin, D. B. (1995) *Biochemistry 34*, 4342−4345.
Pease, E. A., Andrawis, A., & Tien, M. (1989) *J. Biol. Chem. 264*, 13531−13535.
Perie, F. H., & Gold, M. H. (1991) *Appl. Environ. Microbiol. 57*, 2240−2245.
Perie, F. H., Sheng, D., & Gold, M. H. (1996) *Biochim. Biophys. Acta 1297*, 131−148.
Petersen, J. F. W., Kadziola, A., & Larsen, S. (1994) *FEBS Lett. 339*, 291−296.
Piontek, K., Glumoff, T., & Winterhalter, K. (1993) *FEBS Lett. 315*, 119−124.
Poulos, T. L., & Finzel, B. C. (1984) in *Peptide and Protein Reviews* (Hearn, M. T., Ed.) Vol. 4, pp 115−171, Marcel Dekker, New York.
Poulos, T. L., Edwards, S., Wariishi, H., & Gold, M. H. (1993) *J. Biol. Chem. 268*, 4429−4440.
Pribnow, D., Mayfield, M. B., Nipper, V. J., Brown, J. A., & Gold, M. H. (1989) *J. Biol. Chem. 264*, 5036−5040.
Renganathan, V., & Gold, M. H. (1986) *Biochemistry 25*, 1626−1631.
Ritch, T. G., Jr., & Gold, M. H. (1992) *Gene 118*, 73−80.
Schellenberg, K. A., & Hellerman, L. (1958) *J. Biol. Chem. 231*, 547−556.
Schuller, D. J., Ban, N., van Huystee, R. B., McPherson, A., & Poulos, T. L. (1996) *Structure 4*, 311−321.
Sivaraja, M., Goodin, D. B., Smith, M., & Hoffman, B. M. (1989) *Science 245*, 738−740.
Smith, D. W., & Williams, R. J. (1968) *Biochem. J. 110*, 297−301.
Sundaramoorthy, M., Kishi, K., Gold, M. H., & Poulos, T. L. (1994) *J. Biol. Chem. 269*, 32759−32767.
Tuor, U., Wariishi, H., Schoemaker, H. E., & Gold M. H. (1992) *Biochemistry 31*, 4986−4995.
Turano, P., Ferrer, J. C., Cheesman, M. R., Thomson, A. J., Banci, L., Bertini, I., & Mauk, A. G. (1995) *Biochemistry 34*, 13895−13905.
Valli, K., & Gold, M. H. (1991) *J. Bacteriol. 173*, 345−352.
Valli, K., Wariishi, H., & Gold, M. H. (1992) *J. Bacteriol. 174*, 2131−2137.
Vickery, L., Nozawa, T., & Sauer, K. (1976a) *J. Am. Chem. Soc. 98*, 343−350.
Vickery, L., Nozawa, T., & Sauer, K. (1976b) *J. Am. Chem. Soc. 98*, 351−357.
Vitello, L. B., Erman, J. E., Miller, M. A., Mauro, J. M., & Kraut, J. (1992) *Biochemistry 31*, 11524−11535.
Wariishi, H., Akileswaren, L., & Gold, M. H. (1988) *Biochemistry 27*, 5365−5370.
Wariishi, H., Dunford, H. B., MacDonald, I. D., & Gold, M. H. (1989) *J. Biol. Chem. 264*, 3335−3340.
Wariishi, H., Valli, K., & Gold, M. H. (1991) *Biochem. Biophys. Res. Commun. 176*, 269−275.
Wariishi, H., Valli, K., & Gold, M. H. (1992) *J. Biol. Chem. 267*, 23688−23695.
Yonetani, T., & Anni, H. (1987) *J. Biol. Chem. 262*, 9547−9554.

BI962627T